Original

Steinert, N.J.; González-Rouco, J.F.; Melo Aguilar, C.A.; García Pereira, F.; García-Bustamante, E.; de Vrese, P.; Alexeev, V.; Jungclaus, J.H.; Lorenz, S.J.; Hagemann, S.:
Agreement of Analytical and Simulation-Based Estimates of the Required Land Depth in Climate Models.
In: Geophysical Research Letters. Vol. 48 (2021) 20, e2021GL094273.

First published online by AGU: 27.09.2021

https://dx.doi.org/10.1029/2021GL094273

Geophysical Research Letters

RESEARCH LETTER
10.1029/2021GL094273

Key Points:

- Heat conduction from analytical and numerical estimates suggests a required land-model depth of 170 m for climate change simulations
- Agreement between numerical and analytical estimates on climate change timescales gives more confidence for the required land-model depth
- Stepwise land-model depth increase gradually reduces the relative error of shallow models in climate-change simulations

Correspondence to:
N. J. Steinert,
normanst@ucm.es

Citation:
Steinert, N. J., González-Rouco, J. F., Melo Aguilar, C. A., García Pereira, F., García-Bustamante, E., de Vrese, P., et al. (2021). Agreement of analytical and simulation-based estimates of the required land depth in climate models. *Geophysical Research Letters*, *48*, e2021GL094273. https://doi.org/10.1029/2021GL094273

Received 14 MAY 2021
Accepted 27 JUL 2021

Agreement of Analytical and Simulation-Based Estimates of the Required Land Depth in Climate Models

N. J. Steinert[1], J. F. González-Rouco[1], C. A. Melo Aguilar[1], F. García Pereira[1], E. García-Bustamante[2], P. de Vrese[3], V. Alexeev[4], J. H. Jungclaus[3], S. J. Lorenz[3], and S. Hagemann[5]

[1]Complutense University of Madrid, Faculty of Physical Sciences, and Geosciences Institute (UCM-CSIC), Madrid, Spain, [2]Research Center for Energy, Environment and Technology (CIEMAT), Madrid, Spain, [3]Max Planck Institute for Meteorology, Hamburg, Germany, [4]University of Alaska Fairbanks, Fairbanks, AK, USA, [5]Helmholtz-Zentrum Hereon, Geesthacht, Germany

Abstract Previous analytical and simulation-based analyses suggest that deeper land surface models are needed to realistically simulate the terrestrial thermal state in climate models, with implications for land-atmosphere interactions. Analytical approaches mainly focused on the subsurface propagation of harmonics such as the annual temperature signal, and a direct comparison with climate-change model output has been elusive. This study addresses the propagation of a harmonic pulse fitted to represent the timescale and amplitude of anthropogenic warming. Its comparison to land model simulations with stepwise increased bottom boundary depth leads to an agreement between the simulation-based and analytical frameworks for long-term climate trends. Any depth increase gradually decreases the relative error in the subsurface thermodynamics, and a minimum depth of 170 m is recommended to simulate the ground climate adequately. The approach provides an accurate estimate of the required land-model depth for climate-change simulations and assesses the relative bias in insufficiently deep land models.

Plain Language Summary Many current-generation climate models have land components that are too shallow. Under climate change conditions, the long-term warming trend at the surface propagates deeper into the ground than the commonly used 3–10 m. Shallow models alter the terrestrial heat storage and distribution of temperatures in the subsurface, influencing the simulated land-atmosphere interactions. Previous studies focusing on annual timescales suggest that deeper models are required to match subsurface-temperature observations and the classic analytical heat conduction solution. However, for a systematic investigation of land-model deepening in the frame of anthropogenic climate change, the classic analytical solution is inaccurate because it does not mimic the timescale and amplitude of the simulated warming trend. This study intends to bridge the gap between analytical and simulation-based estimates of the subsurface thermodynamic state by adapting the classic analytical framework to mimic long-term anthropogenic warming. The analysis shows that a land-model depth of at least 170 m is recommended for a proper simulation of the post-1850 ground climate, which differs up to 30% from the estimate of the classic approach. Compared to previous studies, this provides an accurate estimate of the required land model depth for long-term climate-change simulations and indicates the relative bias in insufficiently deep land models.

1. Introduction

The thermal state of the ground governs heat and water exchanges, latent and sensible heat fluxes, plant growth rates, and soil organic matter decomposition and transport (e.g., Bonan, 2015; Brubaker & Entekhabi, 1996; Dickinson, 1995; Geiger, 1965; Hillel, 1998; Stieglitz & Smerdon, 2007). Thus, an accurate simulation of the ground thermal regime in Earth system models (ESMs) is important for a more realistic representation of terrestrial ecosystems and land-atmosphere interactions, involving energetic, hydrological, biogeophysical, and agricultural processes relevant for society (e.g., Betts, 2007; Suni et al., 2015).

An important factor influencing the propagation of surface temperature (T_{surf}) variations into the subsurface is the depth of the land surface model (LSM) component in ESMs, which is characterized by the zero-flux bottom boundary condition placement (BBCP). When a temperature signal propagates into the ground

through heat conduction, it experiences an exponential amplitude attenuation and a linear phase shift with depth (Carslaw & Jaeger, 1959). The surface signal affects the subsurface thermal state to a depth at which its amplitude is fully attenuated. This propagation is frequency-dependent. Surface changes reach depths that depend on the timescale of the T_{surf}-signals and on the soil thermal properties such as mineral type and water content that alter the ground thermal diffusivity (Jackson & Taylor, 1986; Sorour et al., 1990).

Despite recent improvements in modeling land surface processes in ESMs (Fisher & Koven, 2020), only limited attention has been directed toward the effect of the BBCP in LSMs and its impact on the representation of terrestrial thermodynamics. Most of the ESMs used in the Coupled Model Intercomparison Project Phases 5 and 6 (CMIP5, CMIP6; Eyring et al., 2016) still have LSMs with a BBCP between 3 and 10 m, with the only exceptions being the CLM and the ORCHIDEE LSMs, extending down to 44 and 90 m, respectively (Burke et al., 2020; Cheruy et al., 2020; Cuesta-Valero et al., 2016).

Analytical estimates of the required BBCP-depth in LSMs can be made by assessing the penetration-depth of simple harmonic sinusoids with varying frequencies into the ground (Alexeev et al., 2007; Smerdon & Stieglitz, 2006). Short-term oscillations of daily and annual periods affect the ground to a depth of about 10 m, whereas decadal to millennial signals can reach several hundred meters (Mareschal & Beltrami, 1992; Pollack & Huang, 2000; Smerdon et al., 2003, 2004). When the penetration-depth of the warming/cooling signal is deeper than the model's BBCP, the heat propagation is unrealistically blocked with subsurface temperatures experiencing enhanced warming/cooling due to a reduced amplitude attenuation with depth (Alexeev et al., 2007; Smerdon & Stieglitz, 2006). Therefore, considering analytical estimates, BBCPs in ESMs are too shallow to represent transient temperature changes like those of historical and scenario simulations.

Additionally, previous studies involving the comparison of climate model output with subsurface temperature profiles (González-Rouco et al., 2009; Stevens et al., 2007) and with estimates of terrestrial energy storage (Beltrami et al., 2006; Cuesta-Valero et al., 2016, 2021; MacDougall et al., 2008, 2010) suggested that models have an unrealistically shallow land representation. Recent developments have also shown that a more realistic subsurface temperature distribution and energy storage capacity are attained when deep BBCPs are considered in historical and stand-alone scenario experiments (González-Rouco et al., 2021; Hermoso de Mendoza et al., 2020; Steinert et al., 2021).

Analytical and numerical approaches address the propagation of temperature changes with depth differently. While the former considers pure harmonic signals and analytical solutions to the infinite half-space heat diffusion (e.g., Alexeev et al., 2007; Smerdon & Stieglitz, 2006; Wang et al., 2016), the latter considers a more realistic climate representation in the boundary conditions used to drive an LSM as it uses a discretization of the heat conduction equation down to the zero-flux BBCP (e.g., González-Rouco et al., 2009, 2021; MacDougall et al., 2008; Smerdon & Stieglitz, 2006; Steinert et al., 2021). The different nature of each framework has likely hampered consistent comparisons between them, although both threads of work have provided compelling evidence for the relevance of using sufficiently deep BBCPs. Differences are most prominent for transient climate signals longer than the oscillations of the daily and seasonal cycles.

This study bridges the gap between these frameworks by considering the consistency of LSMs and analytical schemes to provide sound estimates of the required BBCP-depth in climate models used to simulate long-term climate change. We use an ensemble of simulations of the historical and climate change scenario periods (Eyring et al., 2016) from a state-of-the-art LSM with a progressively increased BBCP-depth, and compare the resulting subsurface temperatures with the analytical representation of a comparable harmonic-type climate change signal. For the first time, an agreement between the simulation-based and analytical frameworks for long-term climate trends can be established by adapting the standard analytical approach to mimic the T_{surf}-signal of the LSM. The results are relevant for the climate modeling community by promoting a more realistic representation of the ground heat storage and exchange and allowing for a refined estimate of the required BBCP-depth in LSM and ESM climate-change simulations.

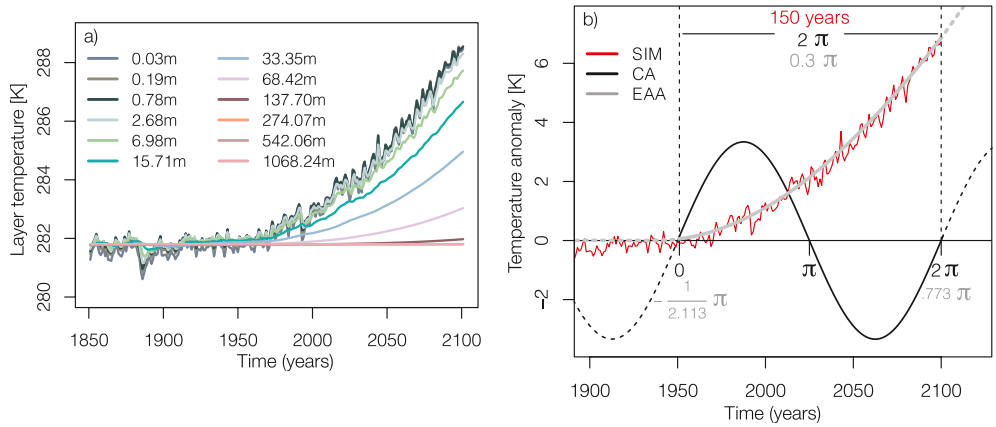

Figure 1. (a) Global mean (no glaciers) temperatures [K] of the historical and RCP8.5 simulated time series (1850–2100) of the deep 12-layer configuration. Subsurface temperatures in JSBACH are calculated at the mid-layer depth. (b) Surface temperature [K] of the historical and RCP8.5 simulations (SIM, red) and idealized harmonic surface temperature pulses for the "Classic Analytical" (CA, black) and the "Effective Adapted Analytical" (EAA, gray) as described in Section 3. Solid lines of the analytical signals indicate the part that is considered for the analysis.

2. Deep Land Surface Model

The LSM used in this study is JSBACH (version 3.20p1; Reick et al., 2021), which is part of the Max Planck Institute Earth System Model (MPI-ESM; Mauritsen et al., 2019) used in CMIP6. In the standard version of JSBACH, the subsurface thermal structure is discretized in five layers, with depths at 0.06, 0.32, 1.23, and 4.13 m, and the BBCP at 9.83 m (Roeckner et al., 2003; Warrilow, 1986). In this study, a modified soil setup with a deeper BBCP (González-Rouco et al., 2021) is used. A simulation with the five-layer standard model is used and additional layers are introduced progressively in seven additional simulations with BBCP-depths at 21.59, 45.11, 91.73, 183.66, 364.47, 719.64, and 1,416.84 m for layers 6 to 12, respectively. The range of depth necessary for timescales investigated herein is expected to be about 200–300 m (Mareschal & Beltrami, 1992; Pollack & Huang, 2000) but prescribing a 1,417 m BBCP allows the deep JSBACH setup to be also used for the simulations of millennial timescales. The subsurface vertical temperature profile is calculated by the one-dimensional heat diffusion equation (Warrilow, 1986), with conduction being the only method of heat transport considered. Soil properties such as the volumetric heat capacity and thermal conductivity are obtained for different soil types from the Food and Agriculture Organization of the United Nations (Dunne & Willmott, 1996) soil map and are constant throughout the soil column in the CMIP6 version of JSBACH. A moisture-dependent thermal diffusivity (Jackson & Taylor, 1986; Sorour et al., 1990) is not represented in the present setup.

LSM simulations (SIM) for eight configurations using 5 to 12 model layers are performed for pre-industrial control conditions (PIC), historical conditions (HIS, 1850–2005), and the 21st-century warming scenario based on the representative concentration pathway RCP8.5 (RCP, 2006–2100; Nakicenovic et al., 2000). JSBACH is run in an offline mode with prescribed atmospheric conditions taken from CMIP5-simulations with the fully coupled MPI-ESM.

The external forcing has a strong influence on the simulated subsurface temperatures with a warming of about 6 K in the top four soil layers (Figure 1a), which is comparable with CMIP5 model estimates (Soong et al., 2020). The high-frequency variability near the surface diminishes in deeper layers because of the frequency-dependent amplitude attenuation. The subsurface temperatures are virtually detached from the T_{surf}-changes below layers 9 and 10 (137.70–274.07 m), which illustrates that a BBCP at 1,417 m is sufficiently deep to resolve the projected 21st-century warming.

3. Classic and Adapted Analytical Heat Diffusion Models

In the "Classic Analytical" (CA) model, the steady-state solution of the one-dimensional heat diffusion equation (Carslaw & Jaeger, 1959), dependent on time and depth z:

$$\frac{\partial T(z,t)}{\partial t} - \kappa \frac{\partial^2 T(z,t)}{\partial z^2} = 0 \tag{1}$$

is

$$T(z,t) = A(z) \cdot sin\left(\frac{2\pi t}{\tau} + \epsilon - \phi(z)\right) \tag{2}$$

using a simple harmonic sinusoid with the temperature T, period τ, thermal diffusivity κ, amplitude $A(z)$, and the phase shift $\phi(z) = dz$, with d being the damping depth $d = \sqrt{\frac{\pi}{\tau\kappa}}$, and the initial phase of the signal oscillation ϵ. The value of κ considered herein is the global mean of JSBACH with $\kappa = 0.79 \cdot 10^{-6} m^2 s^{-1}$.

Depending on the depth of the BBCP, there are two solutions for the amplitude attenuation and the phase shift of the T_{surf}-signal propagating through the ground (Carslaw & Jaeger, 1959; Smerdon & Stieglitz, 2006). One is for an infinite half-space (INF) with a boundary condition at the land surface and a non-limited depth of propagation into the ground. The other solution refers to situations in which the propagation depth is limited by a bottom boundary condition and consequently has limited space (LIM) between the upper and the lower boundaries. For INF, the solutions for A and ϕ take the form:

$$A_{INF}(z) = e^{-dz} \tag{3}$$

and

$$\phi_{INF}(z) = dz. \tag{4}$$

In LIM, they are dependent on the BBCP-depth H (Carslaw & Jaeger, 1959):

$$A_{LIM}(z) = \left(\frac{cosh(2(H-z)d) + cos(2(H-z)d)}{cosh(2Hd) + cos(2Hd)}\right)^{1/2} \tag{5}$$

and

$$\phi_{LIM}(z) = -arg\left(\frac{cosh(d(H-z)(1+i))}{cosh(dH(1+i))}\right). \tag{6}$$

The simple harmonic sinusoids commonly used as T_{surf}-signals in the CA model adequately represent the oscillations of annual temperature cycles. However, this type of function does not represent long-term climate variations of decadal to millennial period length, considering climate change trends seen in recent decades and future projections (IPCC, 2018). Neglecting these longer timescales is potentially problematic when estimating the signal penetration-depth and the associated representation of the subsurface thermal state. Estimates of the required BBCP-depth in LSMs have been established before based on sinusoids of periods τ comparable of the timescales of interest (e.g., Mareschal & Beltrami, 1992; Pollack & Huang, 2000) but no systematic comparison to a realistically deep LSM has been undertaken. The latter is only possible when the characteristics for both the analytical and simulation-based domains are subject to comparable conditions. Therefore, we adapt herein the analytical sinusoid to the simulated T_{surf}-evolution in SIM to obtain an "Effective Adapted Analytical" (EAA) signal that can be used for comparison with the LSM output (Figure 1b).

The CA solution is based on the downward propagation of a sinusoid with a given amplitude that represents the range of the simulated warming and a period that extends over the timescale of warming (Figure 1b; black). As this CA sinusoid does not represent well the pace of warming simulated by SIM, the EAA signal is developed. We use a least-squares regression of a harmonic of the form of Equation 2 to obtain conditions for EAA that are most similar to the simulated T_{surf} (Figure 1b; red). The fit ($r^2 = 0.99$) to the projected warming in the RCP8.5 simulation with a signal period of $\tau = 1000$ years results in a signal amplitude of $A = 14.22$K and an initial phase shift $\epsilon = -\pi/2.11$. Note that changes in the selected period do not affect the results presented herein. The fitted harmonic signal is considered over 0.15 τ of its full period to match the 150 SIM years between 1950 and 2100 (Figure 1b; gray).

In contrast to the CA solution that addresses the attenuation and phase shift of a sinusoid wave, we consider a single sinusoid pulse for EAA as shown in Figure 1b. This mimics the soil thermal behavior in SIM,

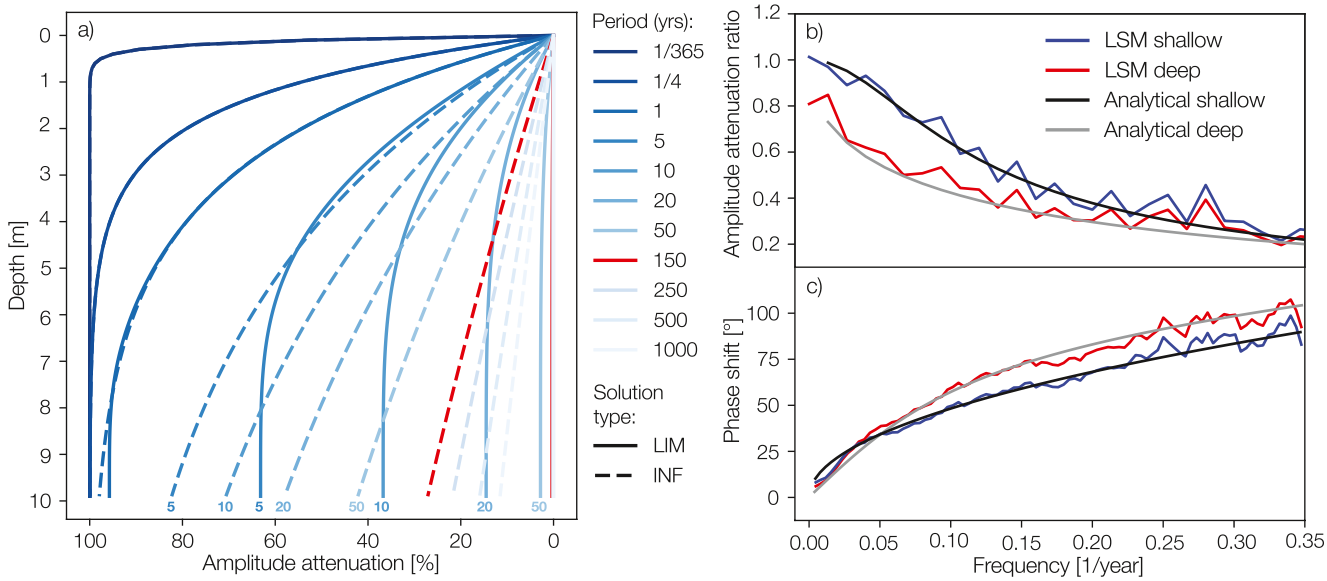

Figure 2. (a) Amplitude attenuation [%] with a depth down to 10 m of different surface signal periods [years] for the infinite half-space solution (INF; dashed lines) and the limited solution (LIM; solid lines) with a bottom boundary condition placement of 10 m depth. (b) Spectral amplitude ratio and (c) cross-phase spectrum between the first (L1) and the fifth (L5) subsurface layers of globally averaged temperatures for the shallow (blue) and deep (red) Land Surface Model simulations and the limited boundary (black) and infinite half-space (gray) analytical solutions. Spectra are calculated from a Welch's periodogram with a 40% "Hamming"-window size and 75% window overlap (Stoica & Moses, 1997).

where T_{surf}-changes are induced into the depth as a gradually changing sinusoid pulse of the timescale of the warming signal. The analytical signal would correspond to a propagating wave, in which previous oscillations that are neglected here would produce an influence on subsurface temperatures. Therefore, the temperature anomaly perturbations at depth are only considered from the moment in time the surface pulse temperature variations reach the respective soil depth. The result is a harmonic function for which subsurface temperatures get influenced solely from the single propagating surface pulse, which closely mimics the mechanism of the LSM. The comparison of the LSM warming trend and the analytical downward propagating pulse is performed by calculating differences between them and with respect to the reference mean state prior to the surface perturbation reaching a given depth.

Following Alexeev et al. (2007), we introduce a temperature error TE to quantify the difference between the solution of the infinite and limited BBCP-depth. The TE-concept can be used in both the LSM and the analytical framework making a direct comparison possible. It reduces the comparison of temperature fields to a function of BBCP-depth H and the T_{surf}-forcing-signal period length τ. We define the temperature difference between two cases with different BBCP-depth as:

$$TE(H,\tau) = \sqrt{\frac{1}{H}\frac{1}{\tau}\sum_{j=1}^{\tau}\sum_{i=1}^{H}\xi = |\overline{T}_{H_d}(z_i,t_j) - \overline{T}_{H_s}(z_i,t_j)|^2\ \Delta z \Delta t}. \quad (7)$$

H_d indicates the model simulation with the deepest BBCP. With a reasonably large BBCP-depth for the corresponding signal period length, $\overline{T}_{H_d}$ can be assumed to resemble the analytical INF solution. Accordingly, H_s describes the simulation with a shallower BBCP ranging from 1 to 1,417 m for the continuous analytical solutions and from 5 to 11 layers for SIM, with $H_{5L} \leq H_s < H_{11L}$ when $H_d = H_{12L}$.

4. Amplitude Attenuation and Phase Shift

The effects of using shallow BBCP-depths in the simulation of the ground thermal state can be illustrated by the differences in the surface signal amplitude attenuation with depth between the analytical LIM and INF solutions (Figure 2a; Equations 3 and 5). For timescales up to the annual cycle, the attenuation percentage is comparable for both LIM and INF, which indicates that a BBCP-depth of 10 m is deep enough for LIM to accommodate such signals. However, for decadal to centennial timescales, the LIM and INF solutions differ

substantially. These signals penetrate deeper into the ground and cannot be represented well by a ground column with a BBCP of 10 m. The two solutions deviate particularly at depths close to the bottom because LIM must satisfy the zero-flux boundary condition at 10 m depth. Differences in the percentage of the attenuation of amplitude range between 19% and 43% for 5- to 250-year signals. For centennial and longer timescales, the physical space in a shallow subsurface is too limited to allow for a significant attenuation in both LIM and INF.

In the following, we apply a spectral analysis (González-Rouco et al., 2009) to explore the amplitude attenuation and phase shift (Equations 3–6) of a surface signal in the ground for the analytical and the LSM frameworks, and to quantify their level of agreement over a range of signal frequencies present in the T_{surf} forcing signal (Figures 2b and 2c). The ratio between the periodogram spectral densities of the first (0.06 m) and the fifth (9.83 m) layer soil temperatures gives a representation of the intensity of amplitude damping (Figure 2b). The shallow LSM (5 layers) performs in good agreement with the analytical LIM solution (Figure 2b; black) over all frequencies but differs substantially from the analytical INF solution (Figure 2b; gray). For short-term periods from 2 to 5 years, the simulations of the deep (1,417 m) and shallow LSM show marginal differences, which suggest that for these signal periods, the shallow LSM is deep enough to simulate a proper temperature distribution. However, for signals of decadal to centennial timescales, there are considerable differences in the amplitude attenuation, which generate crucial temperature differences. In the case of the deep LSM, the simulations are closer to the analytical INF solution, which improves the LSM performance for the subsurface temperature representation. This is also visible in the phase-shift comparison between the deep and shallow models of the analytical and SIM framework. The deep LSM (Figure 2c; red) agrees better with the infinite analytical solution (Figure 2c; gray) with a larger phase shift compared to the shallow solutions, particularly toward the higher frequencies. For long-term signals, the phase-shift differences become smaller until they reverse for frequencies below 0.05 yr^{-1} ($\tau \approx 20$ years). Thus, Figure 2b shows for both the analytical and the numerical LSM approach that a shallow BBCP disrupts the thermal regime and changes how the T_{surf}-signal propagates frequency-dependent in time. Results do not differ in this work if subsurface layer 10 is considered as a representation of the INF detached BBCP case.

5. Agreement of LSM and Analytical Frameworks

Evaluating the differences of the LSM simulated subsurface temperature distribution with the calculation of the *TE* (Figure 3a) for various BBCP-depths H and signal periods τ helps to understand their relationship in the CA framework and identifies combinations that are indicative for a misrepresentation of the ground thermal state. In comparison to Alexeev et al. (2007), we expand the range of signal periods to 1,000 years to cover multi-centennial timescales. For any given signal period, the *TE* is small when the BBCP is close to the surface (Figure 3a). *TE* increases to maximum values of 15%–20% of the T_{surf}-signal amplitude at a BBCP-depth $H_{TE_{max}}$, which shifts to larger BBCP-depth with larger signal periods. The near-surface soil is controlled by the surface forcing and has little thermal inertia because of the limited physical space. The initial *TE*-increase is the net result of a gradually decreasing surface-condition influence toward $H_{TE_{max}}$ and a compensating fraction from the close proximity to the surface boundary. Further increasing the BBCP-depth diminishes *TE* until it converges to zero. The point at which the *TE* becomes nearly zero represents the BBCP-depth that is sufficient for respective H-τ combinations.

A systematic comparison between the analytical solutions (lines) and the model simulations (points) is shown in Figure 3b for the analysis of a cross-section of the *TE*-distribution at a fixed signal period of 150 years (Figure 3a; black line). Note that this 150-year period is the timescale of the CA, EAA, and SIM temperature change in Figure 1b. For CA (Figure 3b; black), the *TE* increases while increasing the BBCP-depth until it reaches a maximum of almost 20% of the T_{surf}-signal amplitude at a model configuration of 25–30 m BBCP-depth. Beyond this depth, the influence of the BBCP decreases in CA with *TE* reaching less than 1% at 120 m. EAA (Figure 3b; gray) shows similar behavior but with important differences. Compared to CA, its maximum values reach *TE* larger than 25% of the T_{surf}-signal amplitude. EAA also shows a different *TE*-trajectory with BBCP-depth, highlighting the relevance of adapting the analytical signal to the sinusoid-pulse for the comparison with the LSM. While it is close to CA for some depth configurations, it differs substantially by up to 35% for others and shows a relative minimum with a BBCP of about 80 m. This shape is independent of the selected κ. EAA's *TE*-convergence to zero is reached at larger BBCP-depth than

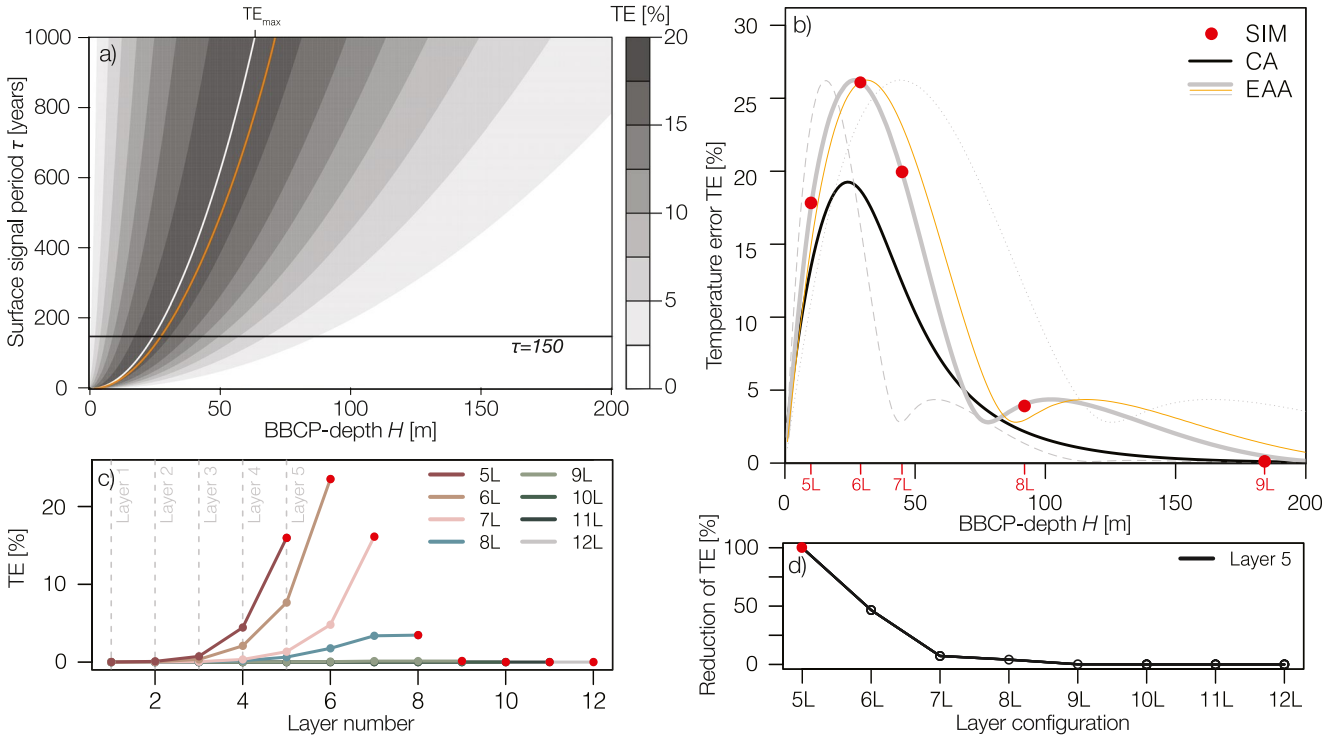

Figure 3. (a) Temperature error *TE* [%] as two-dimensional (time-depth) integrated difference between the analytical solutions for the finite boundary (LIM) and infinite half-space (INF) cases for an idealized harmonic propagating into the ground with dependence to the bottom boundary condition placement (BBCP)-depth H (m) and the surface signal period τ [years]. Each value in the field represents the integrated difference RMSE (Equation 7) between the deep and shallow configurations. Units are given in percentage of the surface signal amplitude. Maximum *TE*-values are indicated for thermal diffusivities of $\kappa = 0.79 \cdot 10^{-6} m^2 s^{-1}$ (white line) and $\kappa = 1.0 \cdot 10^{-6} m^2 s^{-1}$ (orange). The black line indicates a cross-section at $\tau = 150$ years. (b) Temperature error *TE* [%] for the signals of SIM, CA, and EAA in Figure 2a with dependence to the maximum BBCP-depth H [m]. The analytical CA signal (black) represents the *TE*-values between the INF and LIM cases of the cross-section in (a) at $\tau = 150$ years. *TE*-sensitivity for the EAA, INF, and LIM cases to thermal diffusivity values is shown ranging from $\kappa = 0.25 \cdot 10^{-6} m^2 s^{-1}$ (thin gray dashed) over $\kappa = 0.79 \cdot 10^{-6} m^2 s^{-1}$ (thick gray) and $\kappa = 1.0 \cdot 10^{-6} m^2 s^{-1}$ (thin orange) to $\kappa = 2.0 \cdot 10^{-6} m^2 s^{-1}$ (thin gray dotted). Red dots indicate *TE* [%] for the LSM cases. (c) Cumulative *TE* [%] with each layer of the different BBCP-depth configurations of the LSM simulations. Red dots represent the maximum *TE* for a given layer configuration identical with the values in (b). Gray dashed lines indicate layers 1–5 used for the estimation of the relative reduction of *TE* [%]. (d) Relative *TE*-reduction [%] for layer 5 in configurations with 5 layers (5L) to 12 layers (12L) with respect to the 5-layer BBCP configuration. Relative *TE*-reduction in layers 1–4 is comparable to layer 5 and, therefore, not shown.

for CA. For EAA, 170 m BBCP-depth is required for *TE* to become less than 1% compared to 115 m for CA. Thus, using the CA approach, the required BBCP in the LSM is underestimated by 32%.

A direct comparison to SIM (Figure 3b; red points) reveals a good agreement of the *TE*-values of the LSM layer discretization at each BBCP-depth of the EAA solution. Therefore, the *TE*-estimate and the accordingly required BBCP-depth for the LSM can be derived more accurately from the EAA framework and give more realistic results than from the CA case. However, the results are sensitive to variations in the soil thermal diffusivity. Soil with low (high) diffusivity has its maximum *TE* at a smaller (larger) BBCP-depth because the T_{surf}-signal propagates less (more) easily into the ground. Results are shown for soil thermal diffusivities ranging from $0.25 - 2.00 \cdot 10^{-6} m^2 s^{-1}$ with *TE*-values reaching close to zero between 130 and 260 m (Figure 3b; thin gray/orange). The sensitivity illustrates that for different subsurface thermal properties and ground climatic conditions, the required BBCP-depth may vary even for the same T_{surf}-signal.

The fact that the integrated *TE* initially becomes larger while deepening the soil column (e.g., from layer 5 to 6 layer in SIM) is caused by the increase of physical space for the amplitude-attenuation differences to evolve near the bottom boundary. The analysis of the cumulative *TE* (Figure 3c) shows that with a 6-layer configuration of JSBACH (BBCP-depth at 21.59 m), only the absolute *TE* is increased compared to all other depth configurations, while the five uppermost layers (Layer1–Layer5) experience a reduction in *TE* as the BBCP is deepened. Although there is an initial increase of the absolute *TE* when increasing the BBCP, the

relative *TE* in the top five model layers is gradually decreasing by more than 50% each time the BBCP-depth is progressively increased (Figure 3d).

6. Discussion and Conclusions

The results presented herein show agreement between stand-alone numerical LSM simulations and adapted analytical solutions of the heat diffusion equation for long-term climate trends in the case of a shallow and a deep model representation. A comparison using the calculation of the temperature error makes it possible to take advantage of both frameworks. The consistency between the numerical and analytical solutions enables a quantification of the misrepresentation of the subsurface thermal state in too shallow LSMs and provides more confidence in the estimate of BBCP requirements in the land component of state of the art climate models used to simulate long-term climate evolutions.

To reduce the relative integrated temperature error to less than 1%, a minimum BBCP-depth of 170 m is required for 150-year long T_{surf}-signals of the historical and scenario simulations considered herein. However, the results can vary for different soil types and their respective conductive characteristics. BBCP-depth requirements may vary as the same T_{surf}-signal reaches different depths depending on the soil thermal properties. While this is important when looking at specific sites, global LSMs require an average BBCP-depth adequate for any ground conditions and thus are best set to a slightly deeper BBCP to account for ground-type and moisture-content variations. This would increase our estimate of a sufficiently deep BBCP to more than 250 m when the thermal diffusivity is increased from $\kappa = 0.79 \cdot 10^{-6} m^2 s^{-1}$ to $\kappa = 2.0 \cdot 10^{-6} m^2 s^{-1}$.

Although the initial increase of BBCP-depth increases the absolute temperature error, the relative error in the upper 10 m decreases progressively. The increased error may be problematic for climate models that have their BBCP at a critical depth at which the error has its maximum values. However, deepening the soil column may also be an improvement for hydrological or biogeochemical processes (Fisher & Koven, 2020), which generally take place close to the surface, where the relative subsurface thermal state is improved with any increase of the BBCP-depth.

In reality, different soil types and soil-moisture/ice content that can alter the conductive properties of the ground usually occur in the upper 15 m of the subsurface above the bedrock level (e.g., Eliseev et al., 2014). However, some LSMs (such as JSBACH) prescribe constant diffusivity values throughout the ground column at a given grid point that are derived from the near-surface soil characteristics. Although this is helpful for our analysis because the analytical model uses a single diffusivity, it neglects the dynamic influence of soil climatic conditions. An improvement over the approach used herein could be the individual determination of required BBCP-depth for each model grid point, which would account for the spatial variability of static soil thermal properties.

The surface signal propagation into the subsurface depends on the length (period) of the warming signal. Although technically, the penetration-depth does not depend on the strength of the surface warming, its magnitude is important for the detectability of the signal in the subsurface. Hence, model-specific equilibrium climate sensitivity can slightly influence the estimate of penetration-depth from the different magnitude of response to the external forcing. The MPI-ESM is in the lower range of equilibrium climate sensitivity (Meehl et al., 2020) and therefore provides a more conservative example for the projected warming and the required model depth. Our analysis can specifically be adjusted to other models and scenarios by fitting the adapted analytical solution accordingly. Besides using LSM simulations, the adjustment of the EAA signal could also be done based on observational or reanalysis products. Adjusting a harmonic signal to the provided data enables the calculation of the temperature error *TE* and thus, would allow for an evaluation of ground temperatures in a model-data comparison.

Ultimately, the decision on the model depth is a trade-off between computational effort and the remaining temperature error. Increasing the BBCP-depth progressively increases the realism of simulated land surface and subsurface processes. With increased BBCP-depth, however, comes an increased computational effort. In addition to the extra layers to be calculated at each time step, a deeper model requires a longer spin-up time for the soil to reach thermal equilibrium (González-Rouco et al., 2021). Consequently, for temperature trends over longer periods (e.g., millennial timescales), a longer spin-up is necessary. In LSMs with a high

vertical resolution, computational runtime could be increased considerably. From a thermal perspective, sensitivity experiments of higher vertical resolution have shown that the effect on soil temperature trends appears to be minimal (Lawrence et al., 2008; Wang et al., 2016) because the interpolation of the layer thickness increments accounts for the missing layer intervals. However, other soil physical processes may benefit from an increased layer discretization, particularly close to the land surface, where the benefit offsets the compromises in simulation runtime and computational costs.

The presented results provide a refined framework for estimating the required BBCP-depth and its implications for the subsurface thermal regime, which can help the climate modeling community to improve the ground thermodynamic representation in LSM and ESM climate change simulations. The results provide a more accurate estimate of the required land model depth for long-term climate change simulations and assess the relative temperature error in insufficiently deep land models. They further show the sensitivity of heat conduction into the subsurface to variations in the soil thermal properties, which impacts the required BBCP-depth estimates. Due to the sensitivity of the terrestrial heat storage and energy distribution to the vertical design of the ground, most CMIP6 ESMs remain to adjust the depth of their LSM components according to the timescales of interest. However, a demonstration of the effects of using sufficiently deep BBCPs on coupled ESM simulations is still pending.

Data Availability Statement

The associated data sets for this research are available at the DRYAD Digital Repository (doi: 10.5061/dryad.xpnvx0kfn).

Acknowledgments
This work was supported by the projects IlModelS, project no. CGL2014-72659644-R and GReatModelS, project no. RTI2018-102305-B-C21. The work used resources of the Deutsches Klimarechenzentrum (DKRZ) granted by its Scientific Steering Committee (WLA) under project ID bm1026. Vladimir Alexeev was supported by the Interdisciplinary Research for Arctic Coastal Environments (InteRFACE) project through the Department of Energy, Office of Science, Biological and Environmental Research Program's Regional and Global Model Analysis program, and by NOAA project NA18OAR4590417. We also wish to thank Veronika Gayler for technical support on JSBACH and Christian Reick for helpful comments and discussion.

References

Alexeev, V. A., Nicolsky, D. J., Romanovsky, V. E., & Lawrence, D. M. (2007). An evaluation of deep soil configurations in the CLM3 for improved representation of permafrost. *Geophysical Research Letters*, *34*(9), L09502. https://doi.org/10.1029/2007GL029536

Beltrami, H., Bourlon, E., Kellman, L., & González-Rouco, J. F. (2006). Spatial patterns of ground heat gain in the Northern Hemisphere. *Geophysical Research Letters*, *33*(6), L06717. https://doi.org/10.1029/2006GL025676

Betts, R. (2007). Implications of land ecosystem-atmosphere interactions for strategies for climate change adaptation and mitigation. *Tellus Series B: Chemical and Physical Meteorology*, *59*(3), 602–615. https://doi.org/10.1111/j.1600-0889.2007.00284.x

Bonan, G. B. (2015). *Ecological climatology: Concepts and applications* (3rd ed.). Cambridge: Cambridge University Press.

Brubaker, K. L., & Entekhabi, D. (1996). Analysis of feedback mechanisms in land-atmosphere interaction. *Water Resources Research*, *32*(5), 1343–1357. https://doi.org/10.1029/96WR00005

Burke, E. J., Zhang, Y., & Krinner, G. (2020). Evaluating permafrost physics in the Coupled Model Intercomparison Project 6 (CMIP6) models and their sensitivity to climate change. *The Cryosphere*, *14*(9), 3155–3174. https://doi.org/10.5194/tc-14-3155-2020

Carslaw, H., & Jaeger, J. (1959). *Conduction of Heat in Solids* (Vol. 1). Oxford: Clarendon Press.

Cheruy, F., Ducharne, A., Hourdin, F., Musat, I., Vignon, É., Gastineau, G., et al. (2020). Improved near-surface continental climate in IPSL-CM6A-LR by combined evolutions of atmospheric and land surface physics. *Journal of Advances in Modeling Earth Systems*, *12*(10), e2019MS002005. https://doi.org/10.1029/2019MS002005

Cuesta-Valero, F. J., García-García, A., Beltrami, H., González-Rouco, J. F., & García-Bustamante, E. (2021). Long-term global ground heat flux and continental heat storage from geothermal data. *Climate of the Past*, *17*(1), 451–468. https://doi.org/10.5194/cp-17-451-2021

Cuesta-Valero, F. J., García-García, A., Beltrami, H., & Smerdon, J. E. (2016). First assessment of continental energy storage in CMIP5 simulations. *Geophysical Research Letters*, *43*(10), 5326–5335. https://doi.org/10.1002/2016GL068496

Dickinson, R. E. (1995). Land processes in climate models. *Remote Sensing of Environment*, *51*(1), 27–38. https://doi.org/10.1016/0034-4257(94)00062-R

Dunne, K. A., & Willmott, C. J. (1996). Global distribution of plant-extractable water capacity of soil. *International Journal of Climatology*, *16*(8), 841–859. https://doi.org/10.1002/(sici)1097-0088(199608)16:8<841::aid-joc60>3.0.co;2-8

Eliseev, A. V., Demchenko, P. F., Arzhanov, M. M., & Mokhov, I. I. (2014). Transient hysteresis of near-surface permafrost response to external forcing. *Climate Dynamics*, *42*(5–6), 1203–1215. https://doi.org/10.1007/s00382-013-1672-5

Eyring, V., Bony, S., Meehl, G. A., Senior, C. A., Stevens, B., Stouffer, R. J., & Taylor, K. E. (2016). Overview of the Coupled Model Intercomparison Project Phase 6 (CMIP6) experimental design and organization. *Geoscientific Model Development*, *9*(5), 1937–1958. https://doi.org/10.5194/gmd-9-1937-2016

Fisher, R. A., & Koven, C. D. (2020). Perspectives on the future of land surface models and the challenges of representing complex terrestrial systems. *Journal of Advances in Modeling Earth Systems*, *12*(4). https://doi.org/10.1029/2018MS001453

Geiger, R. (1965). *The Climate Near the Ground* (Vol. 93). Cambridge: Harvard University Press.

González-Rouco, J. F., Beltrami, H., Zorita, E., & Stevens, M. B. (2009). Borehole climatology: A discussion based on contributions from climate modeling. *Climate of the Past*, *5*(1), 97–127. https://doi.org/10.5194/cp-5-97-2009

González-Rouco, J. F., Steinert, N. J., García-Bustamante, E., Hagemann, S., de Vrese, P., Jungclaus, J. H., et al. (2021). Increasing the depth of a Land Surface Model. Part I: Impacts on the soil thermal regime and energy storage. *Journal of Hydrometeorology*. https://doi.org/10.1175/JHM-D-21-0024.1

Hermoso de Mendoza, I., Beltrami, H., MacDougall, A. H., & Mareschal, J.-C. (2020). Lower boundary conditions in land surface models—Effects on the permafrost and the carbon pools: A case study with CLM4.5. *Geoscientific Model Development*, *13*(3), 1663–1683. https://doi.org/10.5194/gmd-13-1663-2020

Hillel, D. (1998). *Environmental soil physics*. New York: Elsevier.
IPCC. (2018). Summary for policymakers. In Stocker, T., et al. (Eds.), *Climate change 2013: The physical science basis. Contribution of working group I to the fifth assessment report of the intergovernmental panel on climate change* (pp. 1–30). Cambridge, United Kingdom and New York, NY: Cambridge University Press. Retrieved from www.climatechange2013.org
Jackson, R. D., & Taylor, S. A. (1986). Thermal conductivity and diffusivity. In Klute, A. (Ed.), *Methods of soil analysis: Part 1-physical and mineralogical methods* (Vol. 5.1, pp. 945–956). Soil Science Society of America, American Society of Agronomy. https://doi.org/10.2136/sssabookser5.1.2ed.c39
Lawrence, D. M., Slater, A. G., Romanovsky, V. E., & Nicolsky, D. J. (2008). Sensitivity of a model projection of near-surface permafrost degradation to soil column depth and representation of soil organic matter. *Journal of Geophysical Research*, *113*(F2). https://doi.org/10.1029/2007JF000883
MacDougall, A. H., Beltrami, H., González-Rouco, J. F., Stevens, M. B., & Bourlon, E. (2010). Comparison of observed and general circulation model derived continental subsurface heat flux in the Northern Hemisphere. *Journal of Geophysical Research*, *115*(D12), D12109. https://doi.org/10.1029/2009JD013170
MacDougall, A. H., González-Rouco, J. F., Stevens, M. B., & Beltrami, H. (2008). Quantification of subsurface heat storage in a GCM simulation. *Geophysical Research Letters*, *35*(13), L13702. https://doi.org/10.1029/2008GL034639
Mareschal, J.-C., & Beltrami, H. (1992). Evidence for recent warming from perturbed geothermal gradients: Examples from eastern Canada. *Climate Dynamics*, *6*(3), 135–143. https://doi.org/10.1007/BF00193525
Mauritsen, T., Bader, J., Becker, T., Behrens, J., Bittner, M., Brokopf, R., et al. (2019). Developments in the MPI-M Earth System Model version 1.2 (MPI-ESM1.2) and Its Response to Increasing CO_2. *Journal of Advances in Modeling Earth Systems*, *11*(4), 998–1038. https://doi.org/10.1029/2018MS001400
Meehl, G. A., Senior, C. A., Eyring, V., Flato, G., Lamarque, J. F., Stouffer, R. J., et al. (2020). Context for interpreting equilibrium climate sensitivity and transient climate response from the CMIP6 Earth system models. *Science Advances*, *6*(26), eaba1981. https://doi.org/10.1126/sciadv.aba1981
Nakicenovic, N., Alcamo, J., Davis, G., Vries, B. D., Fenhann, J., Gaffin, S., & Dadi, Z. (2000). *Emissions scenarios—Special report of the intergovernmental panel on climate change*. Cambridge University Press.
Pollack, H. N., & Huang, S. (2000). Climate reconstruction from subsurface temperatures. *Annual Review of Earth and Planetary Sciences*, *28*(1), 339–365. https://doi.org/10.1146/annurev.earth.28.1.339
Reick, C. H., Gayler, V., Goll, D., Hagemann, S., Heidkamp, M., Nabel, J. E. M. S., & Wilkenskjeld, S. (2021). JSBACH 3—The land component of the MPI Earth System Model: Documentation of version 3.2. *Berichte zur Erdsystemforschung*, *240*. https://doi.org/10.17617/2.3279802
Roeckner, E., Bäuml, G., Bonaventura, L., Brokopf, R., Esch, M., Giorgetta, M., & Tompkins, A. (2003). *The Atmospheric General Circulation Model ECHAM 5. PART I: Model Description* (Vol. 349).
Smerdon, J. E., Pollack, H. N., Cermak, V., Enz, J. W., Kresl, M., Safanda, J., & Wehmiller, J. F. (2004). Air-ground temperature coupling and subsurface propagation of annual temperature signals. *Journal of Geophysical Research*, *109*(D21), D21107. https://doi.org/10.1029/2004JD005056
Smerdon, J. E., Pollack, H. N., Enz, J. W., & Lewis, M. J. (2003). Conduction-dominated heat transport of the annual temperature signal in soil. *Journal of Geophysical Research*, *108*(B9), 2431. https://doi.org/10.1029/2002JB002351
Smerdon, J. E., & Stieglitz, M. (2006). Simulating heat transport of harmonic temperature signals in the Earth's shallow subsurface: Lower-boundary sensitivities. *Geophysical Research Letters*, *33*(14), L14402. https://doi.org/10.1029/2006GL026816
Soong, J. L., Phillips, C. L., Ledna, C., Koven, C. D., & Torn, M. S. (2020). CMIP5 models predict rapid and deep soil warming over the 21st century. *Biogeosciences*, *125*(2). https://doi.org/10.1029/2019JG005266
Sorour, M. M., Saleh, M. M., & Mahmoud, R. A. (1990). Thermal conductivity and diffusivity of soil. *International Communications in Heat and Mass Transfer*, *17*(2), 189–199. https://doi.org/10.1016/0735-1933(90)90053-M
Steinert, N. J., González-Rouco, J. F., de Vrese, P., García-Bustamante, E., Hagemann, S., Melo-Aguilar, C., et al. (2021). Increasing the depth of a Land Surface Model. Part II: Sensitivity to improved coupling between soil hydrology and thermodynamics and associated permafrost response. *Journal of Hydrometeorology*. https://doi.org/10.1175/JHM-D-21-0023.1
Stevens, B., Smerdon, J. E., González-Rouco, J. F., Stieglitz, M., & Beltrami, H. (2007). Effects of bottom boundary placement on subsurface heat storage: Implications for climate model simulations. *Geophysical Research Letters*, *34*(2), L02702. https://doi.org/10.1029/2006GL028546
Stieglitz, M., & Smerdon, J. E. (2007). Characterizing land-atmosphere coupling and the implications for subsurface thermodynamics. *Journal of Climate*, *20*(1), 21–37. https://doi.org/10.1175/JCLI3982.1
Stoica, P., & Moses, R. L. (1997). *Introduction to spectral analysis*. Pearson Education.
Suni, T., Guenther, A., Hansson, H. C., Kulmala, M., Andreae, M. O., Arneth, A., et al. (2015). The significance of land-atmosphere interactions in the Earth system—ILEAPS achievements and perspectives. *Anthropocene*, *12*, 69–84. https://doi.org/10.1016/j.ancene.2015.12.001
Wang, F., Cheruy, F., & Dufresne, J. L. (2016). The improvement of soil thermodynamics and its effects on land surface meteorology in the IPSL climate model. *Geoscientific Model Development*, *9*(1), 363–381. https://doi.org/10.5194/gmd-9-363-2016
Warrilow, D. A. (1986). *Modelling of land surface processes and their influence on European climate*. Met 0 20 (Dynamical Climatology Branch), Meteorological Office.